Journal of Applied Sciences

ISSN 1812-5654

science alert

ANSInet
an open access publisher
http://ansinet.com

Journal of Applied Sciences 10 (10): 786-800, 2010
ISSN 1812-5654

Well Logs-Derived Radiogenic Heat Production in the Sediments of the Chad Basin, NE Nigeria

[1]S. Ali and [2]D.M. Orazulike
[1]Physics Programme,
[2]Geology Programme, A.T.B. University, Bauchi, Nigeria

Abstract: Radiogenic heat production estimated from the concentrations of the radioactive elements obtained from log data from a well drilled in the Chad Basin, NE Nigeria range between 0.17 and 1.90, have an average of 0.90±0.01 and a standard deviation of 0.34 μW m^{-3}. The data also indicated that the sediments are low in the concentration of the radioactive element potassium, normal in thorium and higher-than normal in uranium, with potassium contributing only about 7.5% to the production. The Chad, Kerri Kerri, Gombe, Fika, Gongila and Bima Formations are estimated to have average heat productions of 1.02±0.03, 0.62±0.01, 1.21±0.02, 0.93±0.01, 0.94±0.01 and 0.76±0.01 μW m^{-3}, respectively, values observed to be smaller than those of neighbouring basins. Heat production estimated from gamma ray intensity moderately correlated with those estimated from the concentrations of radioactive elements, while only low correlation was observed with heat production estimated from fractional proportion of quartz in matrix. Radiogenic heat is estimated to contribute between 14 and 27% of the surface heat flow, while map view of well site heat production revealed trend that decrease with increasing sediment thickness. Further analysis also suggests that up to 366 m of the bima formation may have been derived from the same source.

Key words: Radiogenic heat production, radioelements, Chad basin, surface heat flow

INTRODUCTION

Radiogenic heat production, RHP, in crustal rocks is dominated by contributions from three radioactive elements, namely uranium, thorium and potassium. These have long half-lives comparable to the age of the earth, sufficient abundance in rocks and have significant proportion of their emissions fully converted to heat within the rocks. Pollack and Chapman (1977) have showed that RHP contributes about 45% of the surface heat flow observed over the continents, while Lachenbruch (1970), Swanberg (1972) and Lowrie (1997) have showed that its magnitude exponential decreases with depth. This decay indicates that RHP comes from a superficial layer of the crust, 4 to 16 km thick, but which averages 10 km. Measurements of RHP show that the acidic rocks have the highest rate of production followed by the basic and ultrabasic ones in that order (Rybach, 1986; Cermak *et al*., 1990; Brown and Musset, 1995). The amount of heat generated by the decay of the radioactive elements of interest depends on the quantities present, their rates of decay as well as the energies of the emissions. Adams and weaver (1958) and Emsley (1998) have established the relative abundance of these elements in rocks. This allows the estimation of the RHP, A_B (μW m^{-3}), by the modified Birch (1954) relationship using 1 below (Beardsmore and Cull, 2001):

$$A_B = 10^{-3} \times \rho(96.7 \times C_U + 26.3 \times C_{TH} + 35.0 \times C_K) \quad (1)$$

where, C_U is the concentration of uranium in parts per million, C_{TH} is the concentration of thorium also in parts per million, C_K is the concentration of potassium in percentage and ρ is the density in g cm^{-3}.

Chapman and Polack (1974) reported values of RHP in the range of 0.96 to 1.8 μW m^{-3} for Precambrian sites on the exposed West African Craton, slightly lower than 1.0 to 3.6 μW m^{-3} for Precambrian sites in Eastern Africa (Chapman and Polack, 1975). Verheijen and Ajakaiye (1979) reported an average RHP of 2.6384±0.8376 nW kg^{-1} ($6.3\pm2.0\times10^{-13}$ cal g^{-1} sec^{-1}) from the younger granite province also on the Precambrian West African Craton. Measurements of RHP in sediments indicates wider variations compared to measurements on Cratons, but with a general decreasing trend from shales through mudstones, sandstones, coals, carbonates and evaporites (Epp *et al*., 1970; Keen and Lewis, 1982; Rybach, 1986; Zhang, 1993; McKenna and Sharp, 1998; Srivastava and Singh, 1998). Ehinola *et al*. (2005) have measured and grouped RHP in the sediments of the

Corresponding Author: S. Ali, Physics Programme, A.T.B. University, Bauchi, Nigeria

Yola arm of the Benue trough, NE Nigeria into low (less than 0.75 nW kg^{-1}), medium (between 0.75 and 1.5 nW kg^{-1}) and high (greater than 1.5 nW kg^{-1}).

The use of Eq. 1 to estimate RHP is dependent on the availability of spectral gamma ray, SGR, readings from rock samples or exposures. More often than not, these data are unavailable. The unavailability of the required data has led to the use of empirical relationships, usually calibrated with A_B. Issler and Beaumont (1986) estimated RHP, A_{IB} (μW m^{-3}), in sediments from the fractional proportion of quartz in matrix, FQ, using Eq. 2:

$$A_{IB} = 1.29 - 0.96 \times FQ \quad (2)$$

Although, RHP in sediments is unconstrained (Beardsmore and Cull, 2001) Eq. 2 yields a heat production of 0.33 μW m^{-3} for pure quartz lithologies and a production of 1.29 μW m^{-3} for quartz-free rocks. Furthermore, Brady *et al*. (2005) have recorded variable RHP from a batholith terrain that has near constant silica content.

Rybach (1986) however, developed a relationship between RHP, A_{BR} (μW m^{-3}) and gamma ray, GR, intensity readings of rocks. This was revised (Bucker and Rybach, 1996) due to the availability of additional data for calibration to Eq. 3:

$$A_{BR} = 0.0158 \times (GR - 0.8) \quad (3)$$

Estimates of A_B by Eq. 1 from Western Australia (Beardsmore and Cull, 2001) and from the Gulf Coast region of Texas (McKenna and Sharp, 1998) have been observed to be significantly less than those obtained using Eq. 3 which, was calibrated using data from one locality. This lack of agreement emphasizes the need for local data in estimating the RHP rather than relying on global averages.

The fact that the GR log is a record of the total emissions from the principal radioactive sources suggest proportionality between GR log on one hand and the SGR logs on the other. The knowledge of the relative activities of the sources (Adams and Weaver, 1958; Emsley, 1998) allowed Beardsmore and Cull (2001) to arrive at the relation:

$$GR \propto POTA + (0.13 \times THOR) + (0.36 \times URAN) \quad (4)$$

where, POTA, THOR and URAN are the SGR readings of the potassium, thorium and uranium logs and all other symbols are as defined earlier.

The proportionality in Eq. 4 is not constant but depends the distance into the rocks that the tool is able to detect the gamma emissions, that is, the radius of influence. The radius of influence however varies with the density of the formation as well as that of the drilling mud filling the hole, with the diameter of the drilled hole, the energy of the emissions and with the tool type (Serra, 1984), but averages 30 cm (Rider, 1991). If, therefore, the radius of influence is the only factor affecting the proportionality, then a plot of GR versus the LHS of Eq. 4 should be approximately linear with a gradient, X, obtained from:

$$GR = X \times [POTA + (0.13 \times THOR) + (0.36 \times URAN)] \quad (5)$$

where, the symbols are as defined earlier.

Dividing Eq. 1 by 5 and re-arranging yields:

$$A_B(\mu Wm^{-3}) = 3.5 \times 10^{-2} \times RHOB \times GR \times \frac{Y}{X} \quad (6)$$

where,

$$Y = \left[\frac{POTA + (0.751 \times THOR) + (2.76 \times URAN)}{POTA + (0.13 \times THOR) + (0.36 \times URAN)}\right]$$

and the other symbols are as defined earlier. Y, called the radiogenic factor, will have values that lie between 1, for the situation when THOR = URAN = 0 and POTA is greater than zero and about 7.67, for the situation when POTA = THOR = 0 and URAN is greater than zero. Beardsmore and Cull (2001) have suggested that the plot of Y should remain invariant with depth for sediments derived from a common source through time.

The availability of gamma ray, spectral gamma ray, SGR, as well as density logs from drilled oil and gas wells has made the estimation of radiogenic heat from well log data an attractive possibility. The purpose of this article is to estimate the radiogenic heat production in the drilled sedimentary formations in the Nigerian Chad Basin using three methods, namely, the method of Birch (1954), the method of Bucker and Rybach (1996) and that of Issler and Beaumont (1986) using well log data. The availability of the estimates of the radiogenic heat production in the sediments will allow for more accurate modelling of the heat flow and basin evolution. It will also allow for more accurate modelling of petroleum maturation and migration within the basin. Furthermore, we will examine the plots of Y versus depth with the aim of determining whether or not the sediments, both at the levels of the drilled column and the formation, are derived from the same environment.

GEOLOGIC SETTING

The Chad basin is one of several basins within the West and Central African rift system and is genetically related to the Benue trough (Burke, 1976). It consists of several sub-basins spread around the republics of Niger, Chad, Cameroon and Nigeria (Genik, 1992). Cratchley (1960) has delineated the Nigerian section into three sub-basins prosperous for hydrocarbons exploration. These are centred around Gubio to the SW, Maiduguri to the South and Lake Chad to the North (Fig. 1). The Bima Formation is the basal unit in a six-unit sequence found in the basin (Fig. 2). The deposition of this sequence of sandstones, mudstones and occasional shales of variable lithology, texture, colour and structure (Carter *et al*., 1963) began in the Aptian to Albian (Genik, 1992) uncomformably on the basement complex. Up to 5 km of this formation have been encountered in drilled holes while interpreted seismic sections suggest 7 to 8 km depth extent (Avbovbo *et al*., 1986). Mudstone and shale horizons within the shallower parts have Total Organic Content (TOC) of between 0.09 and 0.82 wt% (GeoEngineering International, 1994). Sandstones horizons with average of 13.74% (Samaila, 2007) are suggested to form possible reservoirs, while the shale horizons form possible cap and seal rocks.

Overlying the basal Bima is the transitional gongila formation. The deposited of this sequence of fine-to very fine-grained sandstone beds with fair porosity and shale beds, with the beds becoming sandier towards the base, began between the late albian to the early cenomanian in a bi-directional marine transgression across the Tethys from the North and from South Atlantic through the Benue trough to the south (Reyment, 1980; Allix *et al*., 1981; Benkhelil and Robineau, 1983; Genik, 1992). Fossil-rich limestone horizons yielding lower Turonian age also occur towards the base. The formation has abundance of the interbedding of the source, reservoir, seal and cap rocks to from the necessary structures for the entrapment of hydrocarbons. A wholly marine sequence, the Fika Formation, consisting of a sequence of blue-black shales containing one or two thin non-persistent limestone horizons, conformably overlies the Gongila. This was deposited at the height of the marine transgression of the area and may be up to 1000 m thick. Although lacking in reservoir-type rocks, horizons rich in source-type rocks have yielded TOC in the range 0.37 to 1.40 wt% (Robertson Group, 1989, 1991). The end of the transgression was accompanied by the deposition of up 1000 m of a sequence of sandstone, shale, ironstone and coal beds called the Gombe formation over the Fika. This deposition was in an estuarine to deltaic

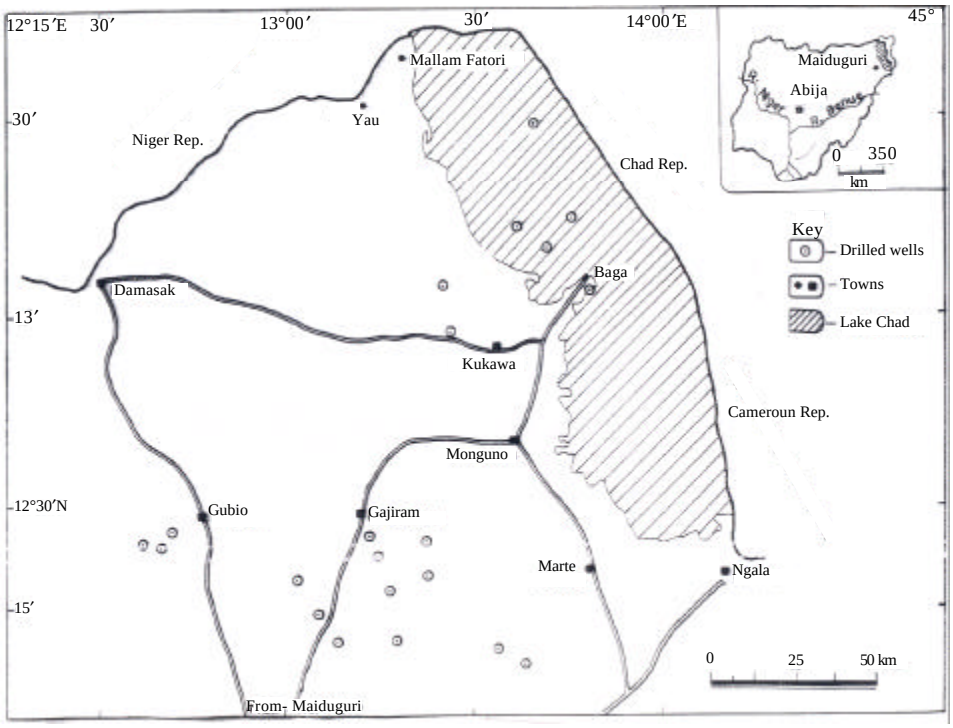

Fig. 1: Location map of the study area

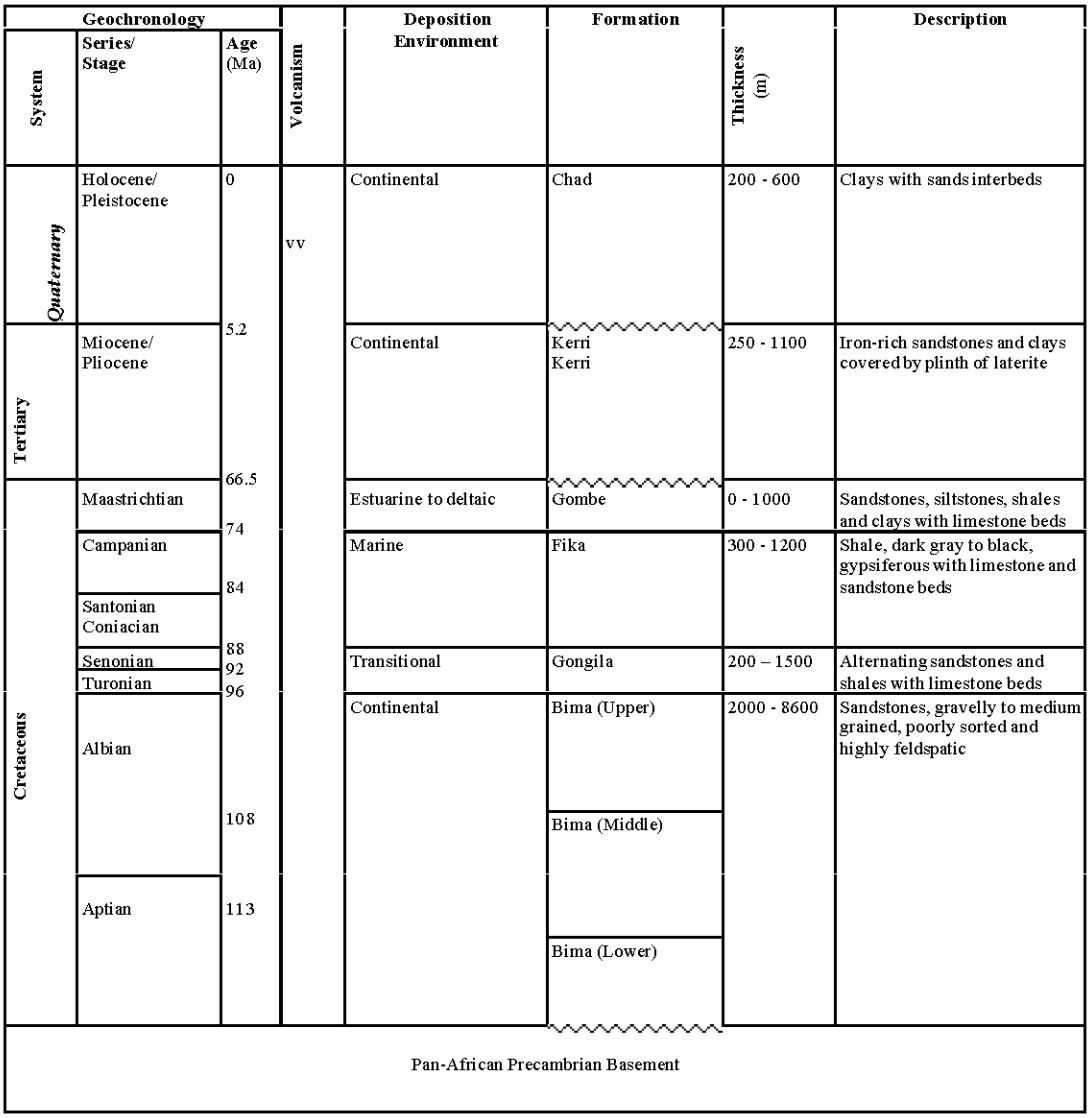

Fig. 2: Generalised stratigraphic column for the Nigerian sector of the Chad Basin

environment, in a minor unconformity. The occurrence of the formation is restricted to the western part of the basin.

A sequence of flat-lying grits, sandstones and clays, deposited by about the late Maastrichtian to the end of Paleocene, that appear to have been derived from a terrain of Cretaceous sedimentary rocks, the Kerri Kerri formation overlie by the Gombe at an angular unconformity. The Chad Formation, a sequence consisting of mostly massive and gritty clays, loosely to uncemented sands and silts overlies the Kerri Kerri Formation at a minor unconformity suggested by seismic data (Avbovbo *et al*., 1986). Its deposition started between middle Neogene to Quaternary times (Carter *et al*., 1963) and lasted till recent times. Intrusive bodies that may be either doleritic or gabbroic, ranging in thickness between five and two hundred and twenty five meters have been found all over the Chad Basin. These have gamma ray intensities of between 20 and 50 API, resistivities of more than 20 ohm m, sonic interval transit times of 230 μsec m^{-1} and less and bulk densities ranging from 2700 to 2900 kg m^{-3}. Similar intrusives have been reported in wells drilled around the Lake Chad in the neighbouring Chad Republic (Genik, 1993).

DATA ACQUISITION

The well log data used in this study were recorded as part of the Chad Basin petroleum exploration-drilling

program of the Nigerian National Petroleum Corporation, NNPC. Five log types were required for the estimation of the radiogenic heat production. These are the gamma ray, GR, bulk density, RHOB, thorium, potassium and uranium spectral gamma ray, THOR, POTA and URAN. The required data were obtained from the Faltu-1 well, drilled to a total depth of 3160 m. The GR log is available from the depth of 50 m to total depth. RHOB log is available from the depth of 550 m to total depth, while the POTA, URAN and THOR logs were available only from the depth of 1360 m to total depth. The scales of the logs allowed the manual picking of the curves at intervals no smaller than 2 m. Further information on the thicknesses of formations at the Faltu-1 well site as well as other drilled well sites was obtained from the report of GeoEngineering International (1994), itself a review of previous studies (Robertson Group, 1989, 1991). The absence of the Gombe Formation in the Faltu-1 well necessitated the search for the relevant data from other wells. The gamma ray logs against the formation from five wells, were obtained. Additional data on shaliness and porosity of the same horizons involved in this study was sought from Ali and Orazulike (2009).

CALCULATIONS, RESULTS AND INTERPRETATIONS

Three sets of RHP estimates were calculated for the drilled horizons in the Faltu-1 well. The first estimates were calculated using the method of Bucker and Rybach (1996). This method requires only the GR log. Estimates of RHP by the method, A_{BR}, were obtained from the depth of 50 m down to total depth. Values of A_{BR} obtained vary between 0.10 and 2.75 μW m^{-3} but averaged 0.91±0.01 μW m^{-3} and have a standard deviation of 0.34 μW m^{-3}. Figure 3 is the plot of A_{BR} versus depth. The red curve and colour-matched equation describe the best fitting polynomial trend of the variation of A_{BR} with depth. The high order and low fit of the equation suggests complex heat generation variation with depth for the drilled horizons. The black curves indicate similar lines for the formations, while Table 1 shows the average A_{BR} for the formations.

The second set of RHP estimates, A_{IB}, was estimated using the method Issler and Beaumont (1986). To estimate the RHP, the method requires the estimate of the fractional proportion of quartz in matrix, FQ. Ali and Orazulike (2009) have estimated both the shaliness and porosity for the depth interval of 50 m to total depth in the Faltu-1 well, the same drilled horizons involved in this study. We made used of the same data to estimate FQ, assuming that the proportion of material remaining after the pores and shales constitute the quartz. The values of A_{IB} obtained vary between 0.36 and 1.16 μW m^{-3} but have an average of 0.66±0.01 μW m^{-3} and a standard deviation of 0.15 μW m^{-3}. Figure 4 is the plot of A_{IB} versus depth. The red curve and colour-matched equation describe the best fitting polynomial trend of the variation of A_{IB} with depth. Similarly also, high order and low fit of the equation suggests complex heat generation variation with depth for the drilled horizons. The black curves indicate similar lines for the formations. Table 1 also shows the average A_{IB} for the formations.

The last set of RHP estimates, A_B, was obtained using the method of Birch (1954). The method requires the SGR logs as well as the bulk density log, RHOB. Although, RHOB log data were available from the depth of 550 m down to total depth, data from the SGR logs were available only from the depth of 1360 m to total depth. Estimates of A_B vary from 0.168 to 1.901 μW m^{-3} and have an average of 0.90±0.01 μW m^{-3} and a standard deviation of 0.34 μW m^{-3} over the depth interval. Figure 5 is a plot of both A_B versus depth. The red curve and colour-matched equation similarly describe the best polynomial trend of the variation of A_B with depth. Here, also high order and low fit of the equation is interpreted to indicate similar scenario. The black curves describe similar lines for the formations while Table 1 also shows the average A_B for the formations. High order polynomial trend with low goodness-of-fit best describe the variations of the three RHP estimates with depth (Fig. 3-5). The order of trends appears to be limited only by the computing power available, in this case the sixth. This is interpreted to indicate diverse RHP from the drilled horizons and hence diverse sedimentation conditions.

Table 1: Average GR, URAN, THOR, POTA log readings and the radiogenic heat productions by the Bucker-Rybach (1996), A_{BR}, Issler-Beaumont (1986), A_{IB} and Birch (1954), A_B, methods in the formations encountered in the Faltu-1 well

Formation	GR API	Density (g cm^{-3})	Uranium (ppm)	Thorium (ppm)	Potassium (%)	A_{BR} (μW m^{-3})	A_{IB} (μW m^{-3})	A_B (μW m^{-3})
Chad	69.72±1.70	-	-	-	-	1.09±0.01	0.66±0.01	1.02±0.03†
Kerri Kerri	42.55±0.92	2.05±0.01	-	-	-	0.66±0.01	0.64±0.01	0.62±0.01†
Gombe	81.13±0.15+	-	-	-	-	1.27±0.01+	-	1.21±0.02†
Fika	62.07±0.83	2.24±0.01	1.85±0.06	8.16±0.19	0.89±0.02	0.97±0.01	0.71±0.01	0.93±0.01
Gongila	69.09±1.00	2.37±0.01	1.76±0.06	5.73±0.15	2.18±0.03	1.08±0.01	0.69±0.01	0.94±0.01
Bima	53.40±1.14	2.49±0.01	1.39±0.06	3.88±0.12	1.90±0.04	0.83±0.01	0.53±0.01	0.76±0.01
column	58.45±0.54	2.25±0.01	1.72±0.04	6.50±0.12	1.51±0.02	0.91±0.01	0.66±0.01	0.90±0.01

Values marked (+) were calculated from gamma ray log from other wells where the Gombe Formation was encountered, while those marked (†) were calculated from the correlation relation between GR log and A_B for deeper formations

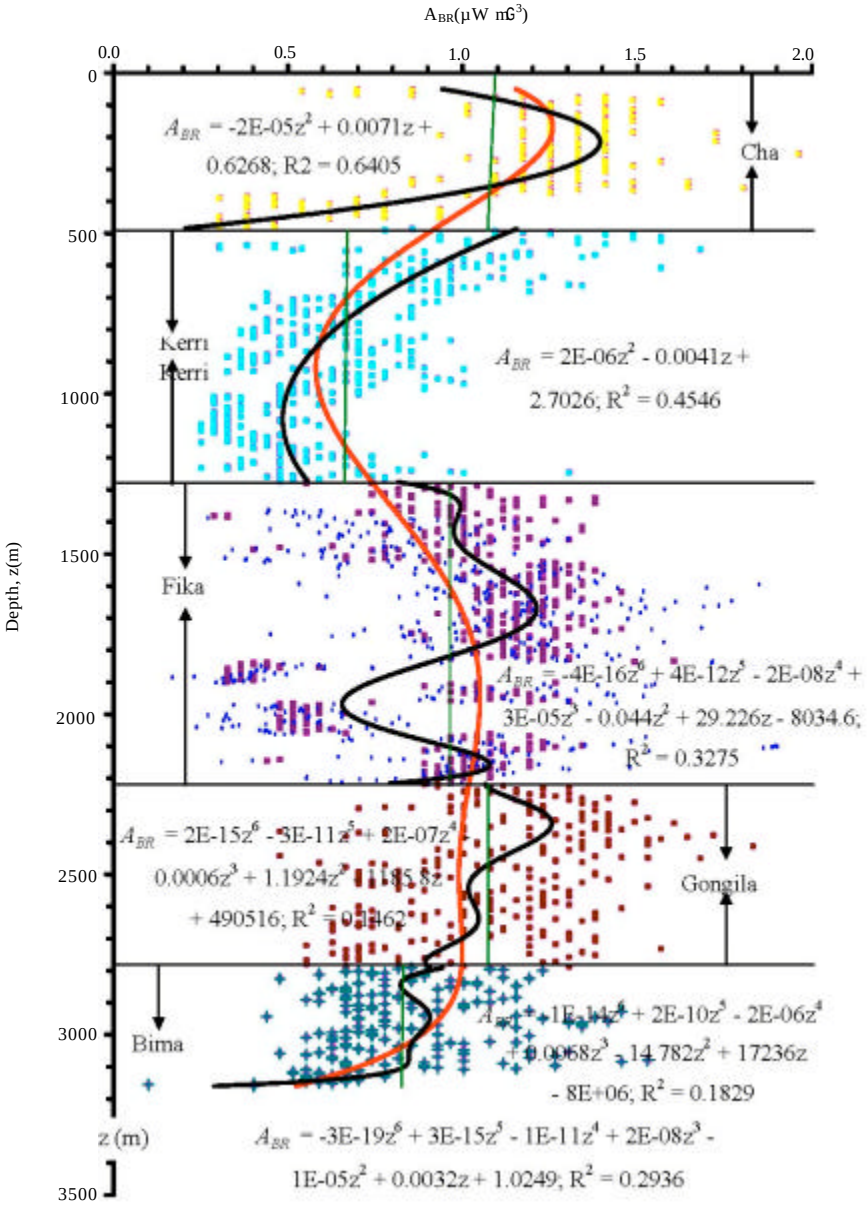

Fig. 3: Plot of Depth, z, versus A_{BR}

Correlation of GR intensity with A_B (Fig. 6) yielded moderate goodness-of-fit which is interpreted to suggest low correspondence between values of the latter from those of the former. In spite of this however, the correlation relation was used to calculate values of A_B for those horizons for which there was insufficient or unavailable data to so directly. Average A_B values marked (†) in Table 1 were obtained using this equation. Furthermore and along with GR logged against the Gombe Formation at other drilled wells, the correlation relation was also used to calculate its average A_B. The cross correlation of A_{BR} against A_B (Fig. 7) also revealed a moderate fit, similar in value to that between GR and A_B and therefore is similarly interpreted. The similarity in the two values of fits is seen as indicating duplication in the two correlations. The cross correlation of A_B and A_{BR} on one hand against A_{IB} on the other (Fig. 8) however reveals low goodness-of-fits for the two situations. This is interpreted to indicate dismal correspondence between values of A_B and A_{BR} predicted from those of A_{IB}. This also questions the estimates of fractional proportion of quartz in matrix, FQ, assumed to be the material that

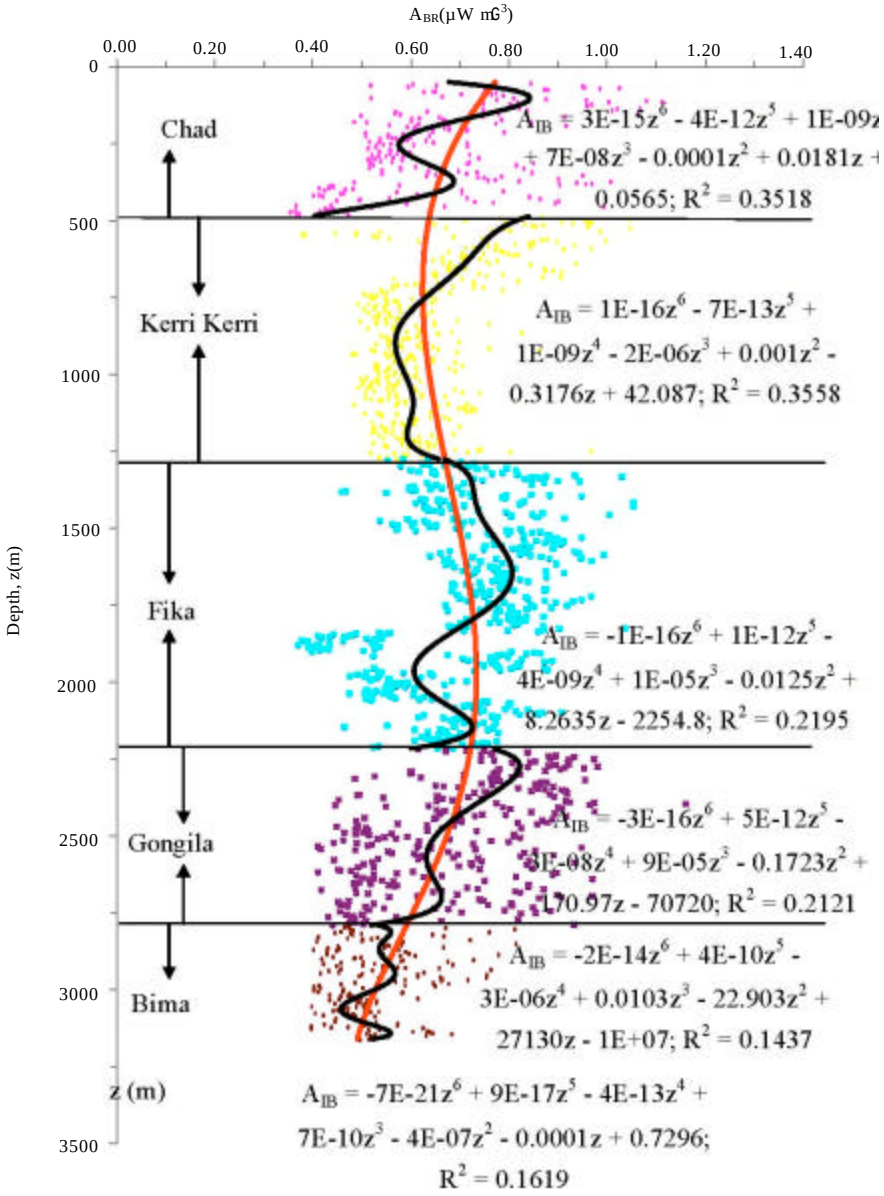

Fig. 4: Plot of Depth, z versus A_{IB}

remains after shale and pores are accounted for and suggest further mineralogical subdivision is needed to more accurately account for the quartz. The correlation of FQ and A_B (Fig. 9) revealed low goodness-of-fit similar in value to that between A_{IB} and A_B.

The assumption of the average A_B in the formations remaining constant over its entire lateral extent, coupled with information on the thicknesses of the formations allowed for the estimation of the total A_B at well sites. For drilled wells for which no information on the thicknesses of formations were available, the average A_B in the Faltu-1 well was multiplied with the total depth of the well to obtain its total A_B. The map view of the result (Fig. 10) reveals total heat production that decreases northward from the south, the general direction of increasing basement depth and thickness of sedimentary profile.

Finally, both at the level of the drilled column (black line) and at levels of the formations (red lines), the plot of the radiogenic factor, Y, versus depth (Fig. 11) reveals only the Bima Formation has depth-invariant linear regression line. This in interpreted to suggest that the 366 m of the formation penetrated in the Faltu-1well are derived from a common source.

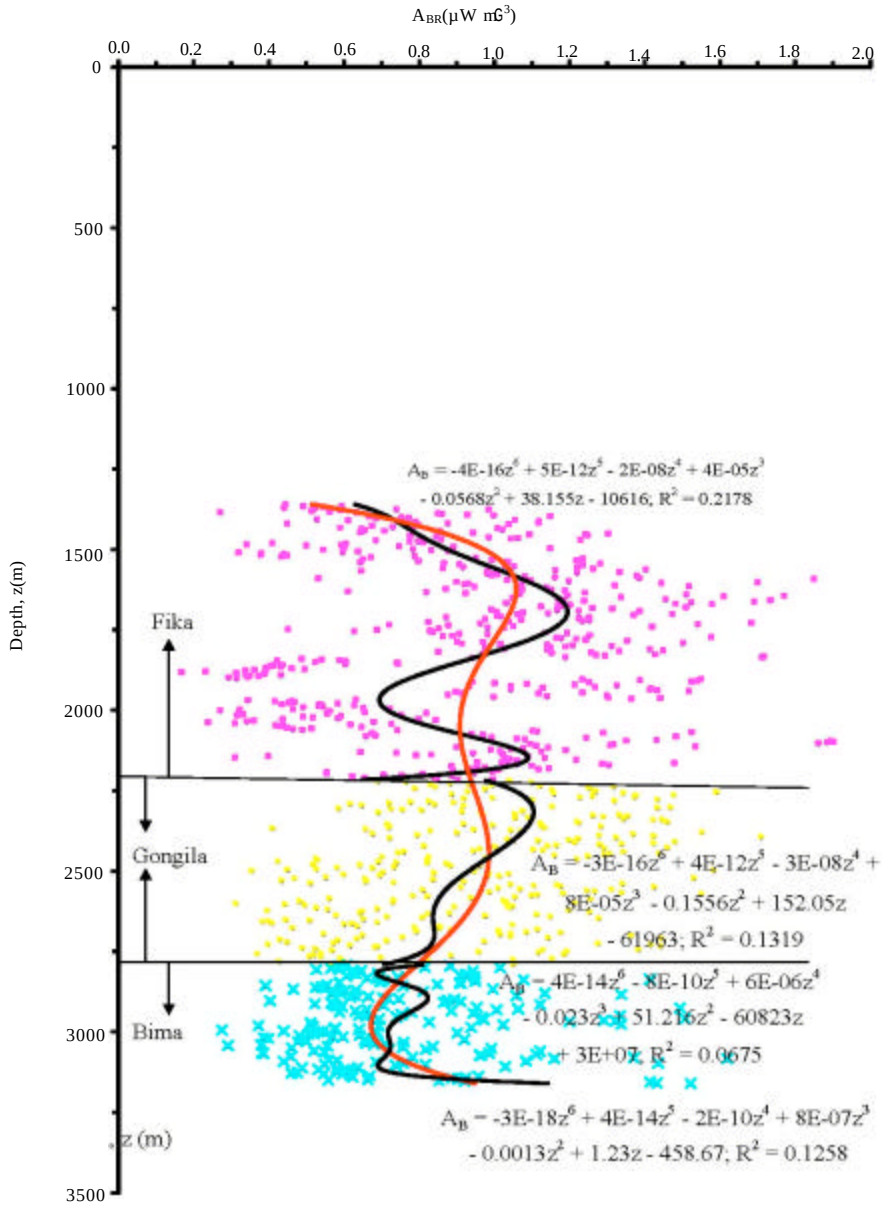

Fig. 5: Plot of Depth, z, versus A_B

SUMMARY AND DISCUSSION

Data from five well logs, gamma ray, bulk density and the spectral gamma rays were sourced from the Faltu-1 well, Chad Basin, NE Nigeria. The data shows that the average intensity of gamma rays within the drilled Chad, Kerri Kerri, Fika, Gongila and Bima Formations are 69.72±1.70, 42.55±0.92, 62.07±0.83, 69.09±1.00 and 53.40±1.14 API respectively, while the average within the drilled column is 58.45±0.54 API. The average gamma radiation intensity is the Gombe Formation is 81.13±0.15 API. While not having readings data against the Chad Formation, the bulk density data shows that the Kerri Kerri, Fika, Gongila and Bima Formations have average densities of 2.05±0.01, 2.24±0.01, 2.37±0.01 and 2.49±0.01 g cm^{-3}. The average bulk density of the drilled column is 2.25±0.01 g cm^{-3}. The spectral gamma ray logs did not have any data against the Chad, Kerri Kerri as well as Gombe Formations. The average concentrations of uranium, thorium and potassium within the remaining Fika, Gongila and Bima Formation are 1.85±0.06 , 8.16±0.19 ppm and 0.89±0.02%; 1.76±0.06, 5.73±0.15 ppm and 2.18±0.03%; and 1.39±0.06, 3.88±0.12 ppm and 1.90±0.04%, respectively. The average concentrations of uranium,

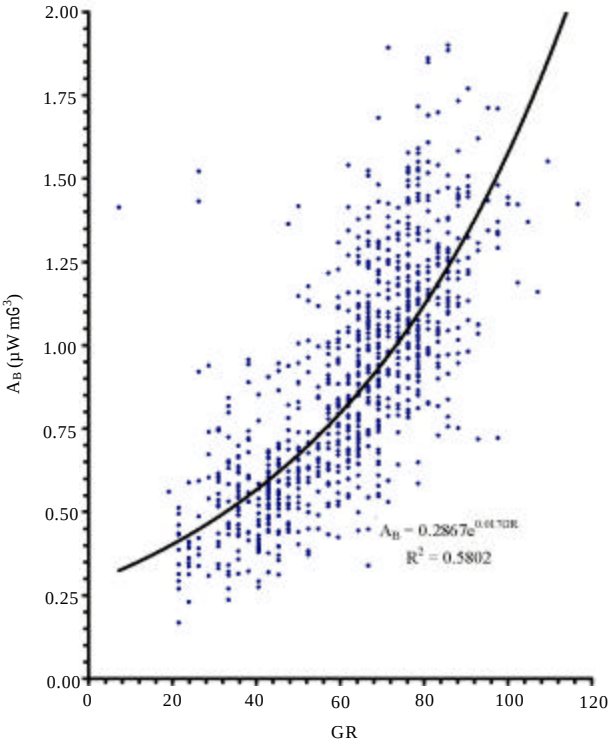

Fig. 6: Plot of GR versus A_B

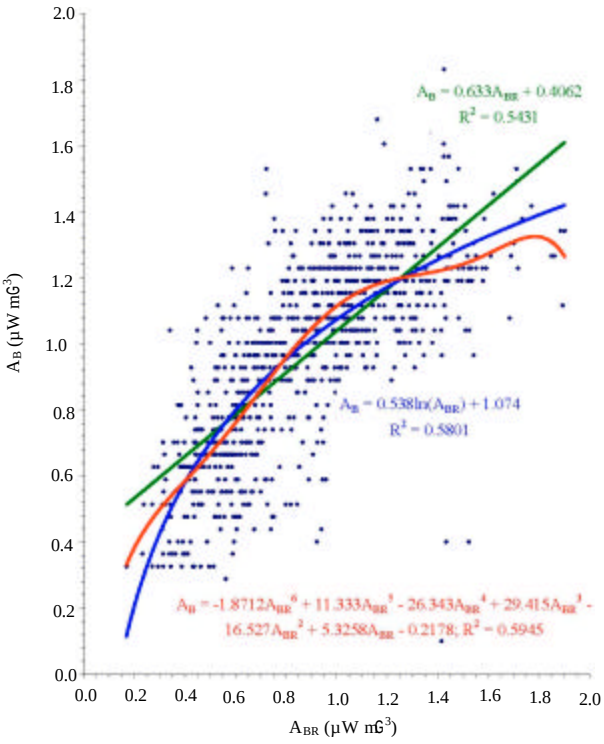

Fig. 7: Cross correlation plot between A_{BR} versus A_B

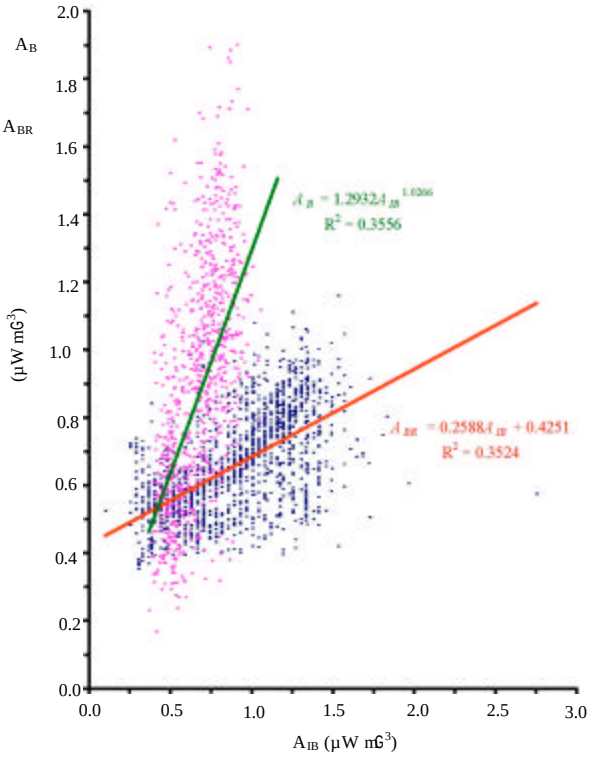

Fig. 8: Cross correlation plots of A_B, A_{BR} versus A_{IB}

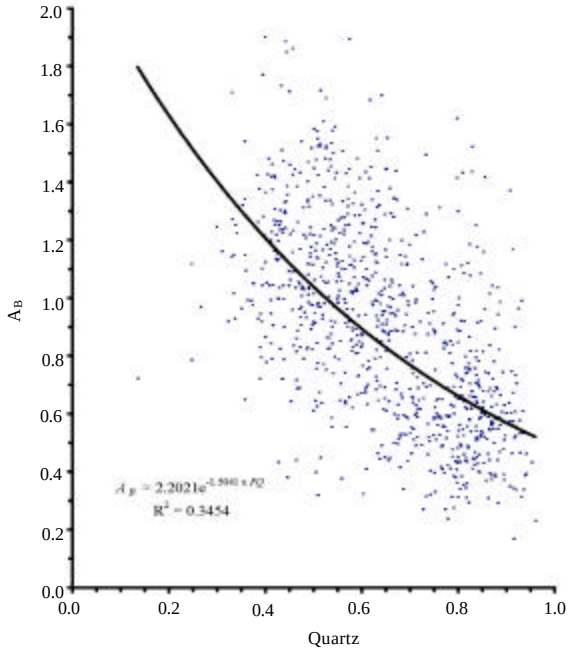

Fig. 9: Correlation of fractional proportion of quartz in matrix, FQ and Birch (1954) radiogenic heat production, A_B

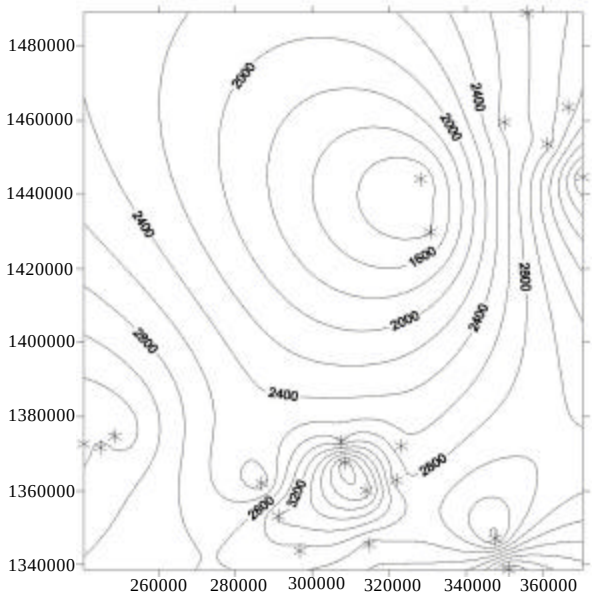

Fig. 10: Map view of well site radiogenic heat production, A_R. Units of contours is $\mu W\ m^{-3}$, contour interval is 100 $\mu W\ m^{-3}$, while the coordinates are in utm

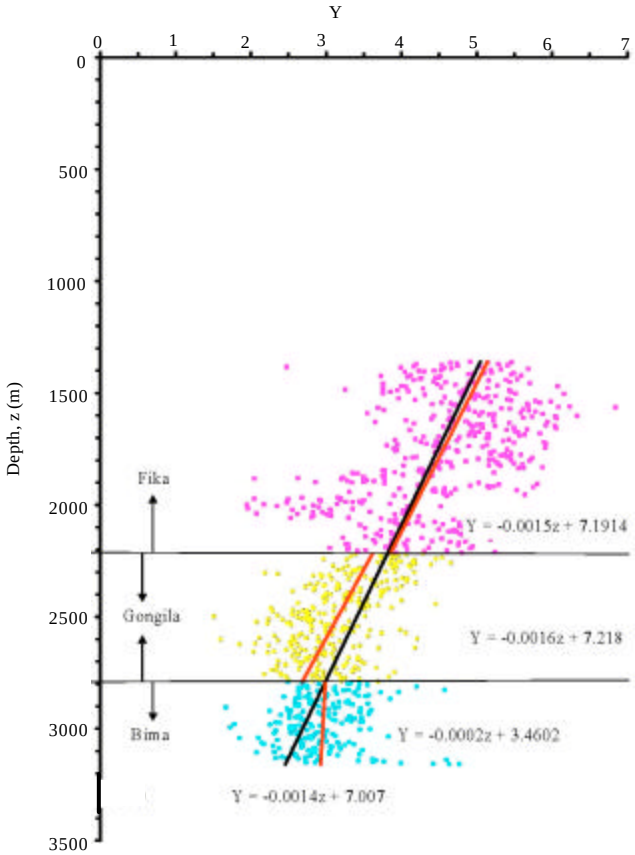

Fig. 11: Depth versus radiogenic factor, Y plot

thorium and potassium within the drilled column are 1.72±0.04, 6.50±0.12 ppm and 1.51±0.02%, respectively.

The radiogenic heat production in the same well was estimated using three different methods adaptable to well log data, namely, the methods of Bucker and Rybach (1996), Issler and Beaumont (1986) and Birch (1954). Estimates of heat production by the Bucker/Rybach method, A_{BR}, vary between 0.10 and 2.75 μW m^{-3}, have an average of 0.91±0.01 μW m^{-3} and have a standard deviation of 0.34 μW m^{-3}. By the same method, the Chad, Kerri Kerri and Fika Formations have average heat productions of 1.09±0.01, 0.66±0.01 and 0.97±0.01 μW m^{-3} respectively, while the Gongila and Bima Formations have productions of 1.08±0.01 and 0.83±0.01 μW m^{-3}. Porosity and shaliness estimates by Ali and Orazulike (2009) were used to estimate heat production by the Issler/Beaumont method, A_{IB} and the estimates vary between 0.36 and 1.16 μW m^{-3} but averaged 0.66±0.01 μW m^{-3} and have a standard deviation of 0.15 μW m^{-3}. The 5 named formations, by the same method, have average productions of 0.66±0.01, 0.64±0.01, 0.71±0.01, 0.69±0.01 and 0.53±0.01 μW m^{-3}, respectively. The estimates of heat production by the method of Birch, A_B, vary between 0.17 and 1.90, have an average of 0.90±0.01 and a standard deviation of 0.34 μW m^{-3}. While not have estimates for the Chad, Kerri Kerri and Gombe Formations, the method has average heat productions of 0.93±0.01, 0.94±0.01 and 0.76±0.01 μW m^{-3} for the Fika, Gongila and Bima Formations respectively. High degree polynomial trends describing the variations of all three RHP estimates with depth were interpreted to indicate diverse sedimentation conditions for the drilled horizons.

Correlation between GR intensities and A_B, although having only a moderate goodness-of-fit of 0.58, allowed the estimation of A_B for the Chad and Kerri Kerri Formations. Along with GR data from other drilled wells in the basin, it also allowed the estimation of average A_B for the Gombe Formation. The cross correlation of A_B and A_{BR} also yielded only a moderate fit, similar in value to that between GR and A_B and interpreted to indicate moderate correspondence between the two heat production estimates. Cross correlation of A_B and A_{BR} on one hand against A_{IB} on the other yielded only low fits which were interpreted to indicate dismal correspondence between the estimates and revealed the need to more accurately account for the proportion of quartz in matrix beyond the simple shale-quartz-pores subdivision. Map view of well site A_B revealed South-North decreasing trend, while plot of the radiogenic factor, Y, revealed that only the 366 m of Bima Formation were derived from the same source.

Uranium in sedimentary rocks originates from acid igneous rocks whose average concentration is about 4.65 ppm (Rider, 1991). Its dispersal into larger space or concentration into smaller space within the basin of deposition means that concentrations in sediments are not constrained, even by its concentration in the parent igneous rocks. McKenna and Sharp (1998) have reported average uranium concentrations of 0.9, 3.7 and 4.0 ppm, respectively for the Stuart City Limestones, Frio Sandstones and Mudstones. Wang *et al*. (2000) have reported values in the range of 0.61 and 3.4 ppm for sediments in the Sichuan Basin, China, while Rolandone *et al*. (2002) have reported averages values of 2.13 and 1.99 ppm, respectively for the Missi sediments and schists of the Hudson Bay area, North America. The pattern of average uranium concentration suggests several inferences. First it suggests decrease in shale content, with the blue-black Fika Formation being the shaliest (Adam and Weaver, 1958; Bjorlykke *et al*., 1975) and closely followed by the Gongila Formation. It also suggests the decreasing percolation of water with depth (Serra, 1979), Fika Formations being the least permeable and the Bima Formation being the most permeable. This is supported by the reversed pattern of density distribution. The slightly lower uranium concentration for the Gongila Formation further suggests the removal of uranium by percolation of subsurface waters. This in turn suggests higher percolation of water in the formation in comparison to the overlying Fika Formation and is interpreted as evidence for the presence of porous and permeable horizons within the formation that may serve as petroleum reservoirs.

The concentrations of thorium in sediments, like those of uranium, are not constrained. However, concentrations ranging between 18 and 26 ppm have been recorded for kaolinite, between 6 and 22 ppm for illite/muscovite, 10 and 24 ppm for smectite and between 2 and 8 ppm for glauconite (Serra, 1979; Dresser Atlas, 1983). McKenna and Sharp (1998) have reported average concentrations of 8.7, 10.6 and 2.1 ppm respectively for the Frio Sandstones and Mudstones as well as the Stuart City Limestones. Wang *et al*. (2000) have reported values in the range of 0.08 and 12.8 ppm, while Rolandone *et al*., (2002) have reported values of 5.37 and 6.13 ppm respectively for Missi sediments and Schists. In comparison therefore, Chad Basin sediments appear to be normal in the radioactive element thorium. The pattern of the distribution of average thorium concentration appears to follow a similar pattern to that of uranium, decreasing with depth. Thorium originates mainly from acid and intermediate igneous rocks and is chemically extremely

stable (Rider, 1991). It will therefore not pass into solution and finds its way into sediments principally as detrital grains, where it is fixed by adsorption (Serra, 1979). Its detrital nature gives it affinity for terrestrial minerals, such as bauxite and kaolinite, over marine ones, such as glauconite (Hassan *et al*., 1976; Dresser Atlas, 1983). The decreasing pattern of average thorium concentration with depth is inferred to reflect similar decrease in kaolinite content.

The concentration of potassium in sediments varies widely, varying from its highest value in illite through glauconite, kaolinite, smectite and chlorite in that order, but averages 2.7% in shales (Serra, 1979; Dresser Atlas, 1983). Wang *et al*. (2000) have reported potassium concentrations in the range of 0.16 and 3.29 % for various sedimentary lithologies in the Sichuan Basin, China, while Rolandone *et al*. (2002) reported average values of 1.83 and 1.06%, respectively for the Missi sediments and schists of the Trans-Hudson Orogen, Canada. McKenna and Sharp (1998) have reported average values of 0.3% for limestones, 2.2% for mudstones and 1.6% for sandstones from offshore Gulf of Mexico. It is thus apparent that the sediments encountered in this study are starved of the radioelement potassium.

The range of A_B estimates encountered in this study is seen to be consistent with that reported by Chapman and Polack (1974) for a Precambrian terrain also in West Africa. The difference between the two may be accounted for by the redistribution of the radioactive elements derived from Precambrian terrain in the process of sedimentation. Using the average density of the drilled sediments of the Faltu-1 well, the average RHP reported by Verheijen and Ajakaiye (1979) converts to a rather high value of 5.936±1.885 μW m^{-3}. Coming from a mine shaft sample however, the high value is not surprising. Similarly also, the RHP classifications of Ehinola *et al*. (2005) convert to less than 1.688 μW m^{-3} for low generating sediments, between 1.688 and 3.375 μW m^{-3} for medium generating sediments and greater than 3.375 μW m^{-3} for high generating sediments. In comparison, the range of A_B for the Chad is smaller, suggesting significant differences in the radiogenic characteristics of the sediments of the Yola arm of the Benue trough from those of the Chad Basin.

The correlation relation between GR and A_B, although with only a moderate fit, provides a relation alternative to that of Bucker and Rybach (1996) for the estimation of RHP for the Chad Basin. This however would need to be subjected to more rigorous tests with data from both drilled wells and from samples. The correlation relation between fractional proportion of quartz in matrix, FQ and A_B also offers alternative relation to that of Issler and Beaumont (1986) for the estimation of RHP. This relation would also need to be similarly tested with data that goes beyond the simple characterization of the lithology into shale-pore-quarzt.

The 3160 m sedimentary profile in the drilled the Faltu-1 well contribute 2682.04 μW m^{-2} to the surface heat flow, while the undrilled section, assumed (Avbovbo *et al*., 1986) to be about 3500 m, would contribute 2660 μW m^{-2}. The total sedimentary profile thus accounts for 5.342 mW m^{-2} of the surface heat flow. If on the basis of Chapman and Pollack (1974) an average surface heat flow of 20 mW m^{-2} is assigned to the basement complex underlying the Chad Basin, then the contribution of the whole sedimentary profile lying on the basement would be about 26.71%. This is similar to the 26% contribution from the sediments of the Gulf Coast region of Texas (McKenna and Sharp, 1998). On the other hand, if on the basis of Verheijen and Ajakaiye (1979), the basement surface heat flow is assumed to be 38.55±1.68 mW m^{-2} (0.92±0.04 HFU), then the contribution of the sedimentary profile would be 13.86%.

Cross correlation of A_B and A_{BR} on one hand against A_{IB} on the other yielded only low fits which were interpreted to indicate dismal correspondence between the estimates and revealed the need to more accurately account for the proportion of quartz in matrix beyond the simple shale-quartz-pores subdivision. Map view of well site A_B revealed South-North decreasing trend, while plot of the radiogenic factor, Y, revealed that only the 366 m of Bima Formation were derived from the same source, in agreement with the suggestion of Carter *et al*. (1963) that the formation constitute three separate formations.

CONCLUSIONS

An examination of the data from the bulk density, gamma and spectral gamma ray logs for the Faltu-1 well, the Chad Basin, NE Nigeria showed that the sediments encountered are starved of the radioelement potassium, normal in the radioactive element thorium and higher-than normal in the concentration of the element uranium. Deficiency of potassium is thought to be linked to kaolinite mineralization prevalent in the Chad Basin, while the pattern of uranium distribution is thought to be linked to subsurface redistribution brought about by the circulation of water. Heat production estimated from the concentrations of the radioactive elements, A_B, range between 0.17 and 1.90, have an average of 0.90±0.01 and a standard deviation of 0.34 μW m^{-3}, with the Chad, Kerri Kerri, Gombe, Fika, Gongila and Bima Formations having average heat productions of 1.02±0.03, 0.62±0.01, 1.21±0.02, 0.93±0.01, 0.94±0.01 and 0.76±0.01 μW m^{-3}

respectively, values smaller than those of sediments from the Yola arm of the Benue trough. While uranium and thorium combine to contribute about 92.5% of A_B, potassium contributes only about 7.5%.

Heat production estimated from gamma ray intensity, A_{BR}, moderately correlated with A_B, while only low correlation was observed between A_B with heat production estimated from fractional proportion of quartz in matrix, A_{IB}, with correlation equations given as $A_B = 0.286 \times e^{-1.017 \times GR}$ and $A_B = 2.202 \times e^{-1.504 \times FQ}$. The drilled section of the sedimentary profile is estimated to contribute 2.682 mW m^{-2} to the surface heat flow, while the undrilled section is estimated to contribute about 2.660 mW m^{-2}. The total sedimentary profile is estimated to contribute between 14 and 27% of the surface heat flow.

Map view of well site heat productions revealed trends that decrease with the general trend of sediment thickness. Analysis of the radiogenic factor, Y, revealed that at least 366 m of Bima Formation may have been derived from the same source.

ACKNOWLEDGMENTS

We wish to acknowledge the Nigerian National Petroleum Corporation, NNPC, for the main data used and for access to many confidential reports. We also thank colleagues in A.T.B. University for comments and criticism that have helped us improve the clarity of some of our arguments. S. Ali, carried out the data collection, analysis and drafted the initial report. D.M. Orazulike participated in the drafting of the report, edited it and agreed with the findings.

REFERENCES

Adams, J.A.S. and C.E. Weaver, 1958. Thorium to uranium ratios as indicators of sedimentary processes: Example of the concept of geochemical facie. AAPG Bull., 42: 387-430.

Ali, S. and D.M. Orazulike, 2009. Petrophysical parameters of sedimentary formations from the Chad Basin, Nigeria estimated using well log data. Global J. Geosci.,

Allix, P.E., E. Grosdidier, S. Jardine, O. Legeox and M. Popoff, 1981. Decouverte daptien superieur a albun inferieur date par microfossiles dans la serie detritique (Nigeria). Comptes Rendus de l Academie des Sciences, 292: 1291-1294.

Avbovbo, A.A., E.O. Ayoola and G.A. Osahon, 1986. Depositional and structural styles in Chad Basin of northeastern Nigeria. AAPG Bull., 80: 1787-1798.

Beardsmore, G.R. and J.P. Cull, 2001. Crustal Heat Flow- A Guide to Measurement and Modeling. Cambridge University Press, Cambridge.

Benkhelil, J. and B. Robineau, 1983. Le fosse de la Benoue est-il un rift?. Bull. Centre Rech. Explor. Prod. Elf Aquitaine, 7: 315-321.

Birch, A.F., 1954. Heat from Radioactivity. In: Nuclear Geology, Faul, H. (Ed.). John Wiley, New York, pp: 148-174.

Bjorlykke K., H. Dypvik and K.G. Finstad, 1975. The Kimmeridge shale, its composition and radioactivity. NFP Jurassic Northern N. Sea Symp. Staranger. Pap., 12: 1-20.

Brady, R.J., M.N. Ducea, S.B. Kidder and J.B. Saleeby, 2005. The distribution of radiogenic heat production as a function of depth in the Sierra Nevada batholith, California. Lithos, 86: 229-244.

Brown, G.C. and A.E. Musset, 1993. The Inaccessible Earth, An Integrated View of its Structure and Composition. 2nd Edn., Chapman and Hall, London, pp: 255-264.

Bucker, C. and L. Rybach, 1996. A simple method to determine heat production from gamma logs. Marine Petroleum Geol., 13: 373-375.

Burke, K.C., 1976. The chad basin: An active intra-continental basin. Tectonophysics, 36: 197-206.

Carter, J.D., W. Barber, E.A. Tait and G.P. Jones, 1963. The geology of parts of Adamawa, Bauchi and Borno provinces in North-eastern Nigeria. Geol. Surv. Nig. Bull., 30: 1-99.

Cermak, V., L. Bodri, L. Rybach and G. Buntebarth, 1990. Relationship between seismic velocity and heat production: Comparison between two sets of data and test of validity. Earth Plan. Sci. Lett., 99: 48-57.

Chapman, D.S. and H.N. Pollack, 1974. Cold spot in West Africa: Anchoring the African plate. Nature, 250: 477-478.

Chapman, D.S. and H.N. Pollack, 1975. Heat flow and incipient rifting in the central African plateau. Nature, 256: 28-30.

Cratchley, C.R., 1960. Geophysical survey of the Southern part of the chad basin. Paper Presented at CCTA Conference on Geology, Kaduna, Northern Nigeria.

Dresser Atlas, 1983. Log Interpretation Chart. Dresser Atlas Publication, Houston, USA.

Ehinola, O.A., E.O. Joshua, S.A. Opeloye and J.A. Ademola, 2005. Radiogenic heat production in the cretaceous sediments of yola arm of nigeria benue trough: Implications for thermal history and hydrocarbon generation. J. Applied Sci., 5: 696-701.

Emsley, J., 1998. The Elements. Oxford University Press, Oxford.

Epp, D., P.J. Grim and M.G. Lamgseth, 1970. Heat flow in the caribbean and gulf of Mexico. J. Geophys. Res., 75: 5655-5669.

Genik, G.J., 1992. Regional framework, structural and petroleum aspects of rift basins in niger, chad and central African republic (C.A.R.). Tectonophysics, 213: 169-188.

Genik, G.J., 1993. Petroleum geology of cretaceous-tertiary rift basins in Niger, chad and central African republic. AAPG Bull., 77: 1405-1434.

Geo Engineering International, 1994. Re-appraisal of the hydrocarbon potential of the Nigerian sector of the Chad Basin. NAPIMS, NNPC, Nigeria.

Hassan, M., A. Hossin and A. Combaz, 1976. Fundamentals of the differential gamma ray log interpretation technique. SPWLA 17th Ann. Symp., Paper 1976-H, pp: 1-18. http://www.onepetro.org/mslib/servlet/onepetropreview?id=SPWLA-1976-H&soc=SPWLA&speAppNameCookie=ONEPETRO.

Issler, D.R. and C. Beaumont, 1986. A Finite Element Model of the Subsidence and Thermal Evolution of Extensional Basins: Application to the Labrador Continental Margin. In: Thermal History of Sedimentary Basins: Methods and Case Histories, Naeser, N.D. and T.H. McCulloh (Eds.). Springer-Verlag, New York, pp: 239-267.

Keen, C.E. and T. Lewis, 1982. Measured radiogenic heat production in sediments from the continental margin of eastern North America: Implications for petroleum generation. AAPG Bull., 66: 1402-1407.

Lachenbruch, A.H., 1970. Crustal temperature and heat productivity: Implications for the linear heat flow relation. J. Geophys. Res., 75: 3291-3300.

Lowrie, W., 1997. Fundamentals of Geophysics. Cambridge University Press, Cambridge, ISBN-13:9780521675963.

McKenna, T.E. and J.M. Sharp, 1998. Radiogenic heat production in sedimentary rocks of the gulf of Mexico basin. AAPG Bull., 82: 484-496.

Pollack, H.N. and D.S. Chapman, 1977. On the regional variation of heat flow, geotherms and lithospheric thickness. Tectonophysics, 38: 279-296.

Reyment, R.A., 1980. Biostratigraphy of the saharan cretaceous and paleocene epicontinental transgression. Cretaceous Res., 1: 299-327.

Rider, M.H, 1991. The Geological Interpretation of Well logs. Whittles Publishing, Scotland.

Robertson Group, 1989. The stratigraphy, sedimentology and geochemistry of the NNPC Tuma-1, Sa-1 and Kanadi-1 wells, drilled in the Nigerian chad basin, borno state, Nigeria. NNPC, Lagos, Nigeria. Report 4084/Ib.

Robertson Group, 1991. The stratigraphy, sedimentology and geochemistry of the NNPC Ngamma East-1 and Gubio SW-1 wells, drilled in the Nigerian chad basin, borno state, Nigeria and correlation with the previously studied Tuma-1, Kanadi-1 and Sa-1 wells. NNPC, Nigeria Report 4531/Ib.

Rolandone, F., C. Jaupart, J.C. Mareschal, C. Gariepy, G. Bienfait, C. Carbonne and R. Lapointe, 2002. Surface heat flow, crustal temperatures and mantle heat flow in the proterozoic trans-hudson orogen, Canadian shield. J. Geophys. Res., 107: 2341-2341.

Rybach, L., 1986. Amount and Significance of Radioactive Heat Sources in Sediments. In: Collection Colloques Seminares 44, Thermal Modelling of Sedimentary Basins, Burrus, J., (Ed.). Paris Editions Technip, Paris, pp: 311–322.

Samaila, N.K., 2007. Reservoir potentials of the upper bima sandstone in the yola and lau-lamurde basins, upper benue trough, NE Nigeria. Ph.D. Thesis, Geology Programme, A.T.B. University, Nigeria.

Serra, O., 1979. Diagraphies Differies: Bases De L' Interpretation Tome 1: Acquisition Des Donnees Diagraphiques. Elf-Acquitaine, Paris, pp: 328.

Serra, O., 1984. Fundamentals of Well-Log Interpretation: I. The Acquisition of Logging Data. Elsevier, Amsterdam, Netherlands.

Srivastava, D.N. and R.A. Singh, 1998. Possibility of fractal growth in polymer composites of charge-transfer materials. Synthetic Metals, 96: 235-238.

Swanberg, C.A., 1972. Vertical distribution of heat generation in the Idaho batholith. J. Geophys. Res., 77: 2508-2513.

Verheijen, P.J.T. and D.E. Ajakaiye, 1979. Heat flow measurements in the Ririwai ring complex, Nigeria. Tectonophysics, 54: T27-T32.

Wang, X., J. Wang, Q. Li and H. Yu, 2000. Deep heat flow and geothermal structure in sichuan basin of China. Proceedings of the World Geothermal Congress, May 28-June 10, Kyushu-Tohoku, Japan, pp: 1-4.

Zhang, Y.K., 1993. The thermal blanketing effect of sediments on the rate and amount of subsidence in sedimentary basins formed by extension. Tectonophysics, 218: 297-308.